Kovove Mater. 49 2011 197–205
DOI: 10.4149/km_2011_3_197

Enhancing overall tensile behavior or ductility of AZ91D using nano-Al_2O_3 and heat treatment

M. Shanthi, K. S. Tun, R. S. Pandey, M. Gupta*

Department of Mechanical Engineering, National University of Singapore, 10, Kent Ridge Crescent, Singapore-119260

Received 23 September 2010, received in revised form 29 September 2010, accepted 1 October 2010

Abstract

In the current study, magnesium based nanocomposites containing 1 and 1.5 vol.% alumina particulates as reinforcement were synthesized using a disintegrated melt deposition technique. Microstructural characterization of the composite materials revealed uniform distribution of Al_2O_3, good interfacial integrity between the matrix and reinforcement and presence of limited porosity. Mechanical properties characterization results revealed that the presence of nano-Al_2O_3 reinforcement led to an improvement in hardness, 0.2 % yield strength, UTS, ductility and work of fracture. Solutionizing heat treatment carried out at a temperature of 413 °C for 2 h led to a significant enhancement in ductility of the nanocomposites (31 % ductility exhibited by AZ91D/1.5 Al_2O_3). This study clearly reveals the ability of Al_2O_3 particulates and solutionizing heat treatment to vary the tensile response of AZ91D/Al_2O_3 nanocomposites enabling them to be used in a wide spectrum of engineering applications.

K e y w o r d s: AZ91D, nano-alumina, solutionizing heat treatment, mechanical properties, microstructure

1. Introduction

Magnesium and its alloys have become promising materials for portable electronic devices, aircraft and automobile industries due to their attractive properties such as low density, high specific strength, high damping capacity and good electrical and thermal conductivity [1–3]. Major limitations of magnesium and its alloys include low ductility, low elastic modulus [4], poor corrosion resistance and susceptibility to premature failure at high temperatures (creep).

AZ91D is one of the widely used magnesium alloys as it offers a good combination of mechanical and physical properties with low cost and is preferred for the production of lightweight vehicles in the automotive industry. However, the usage of this alloy is limited below 150 °C because of its poor creep resistance and tensile properties at elevated temperatures. To improve these mechanical properties, researches have been carried out by alloying magnesium with elements such as Ca, Sr, Bi, Sb and Y [5–8]. Yuan et al. [5] reported improved yield strength and creep resistance at elevated temperature up to 200 °C by the addition of Bi and Sb alloying element to AZ91 magnesium alloy. Wu et al. [7] reported the combined effect of Ca and RE elements on improving the UTS of AZ91D alloy. Zhao et al. [8] reported that alloying AZ91D with Y led to an improvement in tensile strength, yield strength and elongation of AZ91D alloy. A number of investigations have also been made to study the corrosion resistance [9, 10] and fatigue behaviour of AZ91D alloys [11].

Apart from alloying technique, few attempts have also been made to study the potential of magnesium based composites containing either particles or fibers. These composites have showed significant increase in mechanical properties [11–14]. For example, the use of SiC particulate reinforcement ($\sim$ 7–25 μm) increases the stiffness, dimensional stability, specific strength at room and elevated temperatures, damping capability and creep properties of magnesium [14–16]. However, these composites exhibited poor ductility. Results of literature survey indicate that no attempt has been made so far to reinforce AZ91D alloy using cost effective, thermally stable and stiff alumina particulates in nano-length scale using solidification

*Corresponding author: tel.: +65 6516 6358; fax: +65 6779 1459; e-mail address: mpegm@nus.edu.sg

processing technique and to investigate the properties of such nanocomposites under solutionized condition.

Accordingly, the main aim of the current study was to synthesize AZ91D/Al_2O_3 nanocomposites using disintegrated melt deposition technique. The effect of nano-alumina particulate addition and solution heat treatment on the microstructural evolution and mechanical properties of the composites were investigated. An attempt was also made to compare the mechanical properties of AZ91D and its composites under non-heat treated and heat treated conditions.

2. Experimental procedures

2.1. Primary processing

2.1.1. Materials

In this study, AZ91D magnesium alloy ingots with chemical composition of (8.3–9.7 % Al, 0.15 % Mn, 0.35–1.0 % Zn, 0.1 % Si, 0.005 % Fe, 0.03 % Cu and 0.001 % Ni) were cut into 4 cm square blocks. Holes of 8 mm diameter were drilled into these blocks and required amount of 50 nm alumina particulates (supplied by Baikowski, Japan) were filled in these holes. Two different volume percentages (1.0 and 1.5 %) of nano-alumina particulates were chosen as reinforcements for AZ91D magnesium alloy.

2.2.2. Disintegrated melt deposition technique

Synthesis of monolithic and AZ91D/Al_2O_3 nanocomposites containing two different volume fractions of alumina was carried out using DMD technique. It involves the melting and superheating of AZ91D blocks with nano-alumina reinforcement particulates to 750 ℃ under inert Ar gas atmosphere in a graphite crucible using the resistance heating furnace. The molten slurry was stirred at 460 rpm for 2.5 min using a zirtex coated twin blade (pitch 45°) stirrer to facilitate the incorporation and uniform distribution of reinforcement particulates in the metallic melt. The melt was then released through a 10 mm diameter orifice at the base of the crucible and was disintegrated by two jets of argon gas orientated normal to the melt stream. The disintegrated composite melt slurry was subsequently deposited onto a metallic substrate located 500 mm from the point of disintegration, forming ingots of 40 mm diameter. The synthesis of monolithic AZ91D alloy was carried out using the same procedure for comparison purpose. Solutionizing heat treatment was carried out at a temperature of 413 ℃ for 2 h [17] followed by quenching (25 ℃) for monolithic AZ91D and AZ91D/Al_2O_3 nanocomposites to study the effect of heat treatment on the mechanical properties.

2.2. Secondary processing

The cast ingots obtained from the primary processing were machined to 36 mm diameter and 40 mm height billets. The billets were hot extruded at 350 ℃ employing an extrusion ratio of 20.25 : 1 using a 150 ton hydraulic press. These billets were soaked at 400 ℃ for 1 h before extrusion. Colloidal graphite was used as lubricant during extrusion. Rods of 8 mm diameter were obtained after extrusion and used for further characterizations.

2.3. Density measurement

Density was measured using the Archimedes' principle on three randomly selected samples of AZ91D alloy and AZ91D/Al_2O_3 nanocomposites. Distilled water was used as the immersion fluid. The weight of the samples was measured in air and water using an A&D ER-182A electronic balance, with an accuracy of ± 0.0001 g.

2.4. Microstructural characterization

Microstructural characterization studies were conducted on polished samples to investigate the size and morphology of grains, distribution of secondary phases and reinforcement within the matrix and interfacial integrity between the matrix and reinforcement. The OLYMPUS optical microscope, Scion Image Analyzer and Hitachi S-4300 Field Emission Scanning Electron Microscope (FESEM) equipped with EDS were used for characterization.

2.5. X-ray diffraction

X-ray diffraction analysis was carried out on non-heat treated and heat treated AZ91D/Al_2O_3 nanocomposites. Automatic Shimadzu XRD-6000 diffractometer was employed to identify the phases present in the materials. The samples were exposed to Cu Kα radiation (λ = 1.54056 Å) at a scanning speed of 2 deg min^{-1}.

2.6. Hardness

Microhardness measurements were made on the polished AZ91D and AZ91D/Al_2O_3 samples. The Vickers' microhardness was measured using Matsuzawa MXT50 automatic digital microhardness tester in accordance with ASTM E384-99 standard.

2.7. Tensile testing

Room temperature tensile properties of extruded AZ91D and AZ91D/Al_2O_3 samples were determined in accordance with ASTM test method E8M-05 using

Table 1. Results of density and porosity measurements of non-heat treated AZ91D and AZ91D/Al_2O_3 nanocomposites

Specimen	Density ($g\,cm^{-3}$)		Porosity (%)
	Theoretical density	Experimental density	
AZ91D	1.81	1.8102 ± 0.0012	0.00
AZ91D/1.0Al_2O_3	1.8315	1.8144 ± 0.0020	0.93
AZ91D/1.5Al_2O_3	1.84225	1.8178 ± 0.0056	1.33

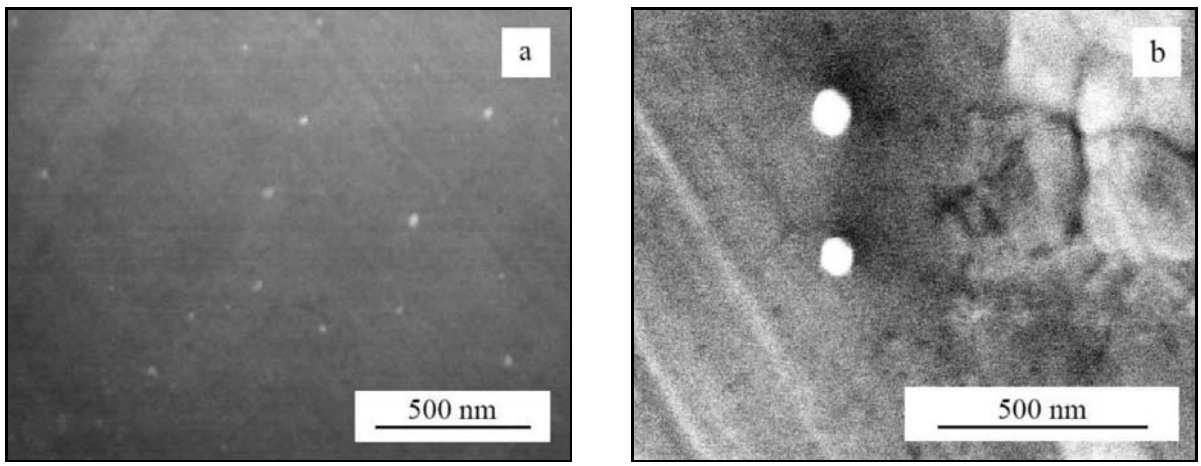

Fig. 1. Representative FESEM micrographs showing: (a) distribution of Al_2O_3 nano-particulates and (b) interfacial characteristics of AZ91D alloy and alumina particulates in case of AZ91D/1.5Al_2O_3 nanocomposite.

MTS 810 tensile testing machine with a cross-head speed set at 0.254 mm min^{-1} on round tension test specimens of 5 mm diameter and 25 mm gauge length. MTS type extensometer was used for strain recording.

2.8. Fractography

Fractography was carried out on the surface of fractured tensile samples using Hitachi S4300 Field Emission Scanning Electron Microscope (FESEM).

3. Results

3.1. Macrostructural characteristics

Macrostructural characterization conducted on the as deposited monolithic magnesium and its composites did not reveal any shrinkage cavity and the presence of macropores. Extruded 8 mm rods of AZ91D and AZ91D/Al_2O_3 nanocomposites also did not reveal any macrostructural defects.

3.2. Density measurements

The results of density measurements are shown in Table 1. The near dense monolithic and composite samples fabricated from the current study are supported by the observation of minimal porosity (> 98 %) in the samples (Table 1).

3.3. Microstructural characteristics

Microstructural characterization conducted on the non-heat treated nanocomposite specimens showed near equiaxed grain morphology, reasonably uniform reinforcement distribution (Fig. 1a) with good interfacial integrity between the matrix and reinforcement (Fig. 1b) and uniformly distributed intermetallic particulates in AZ91/1.5vol.%Al_2O_3 samples as shown in Fig. 2b. After heat treatment, the microstructural characterization of the nanocomposites revealed increased grain size (Table 2), and fine intermetallic particulates uniformly distributed in the matrix (Fig. 2d).

3.4. X-ray diffraction

Figure 3 shows X-ray diffractograms obtained from non-heat treated and heat treated AZ91/1.5vol.% Al_2O_3 nanocomposites. Diffractograms show the presence of intermetallic β-$Al_{12}Mg_{17}$ phase and α-Mg phase in non-heat treated samples and only α-Mg phase in heat treated samples.

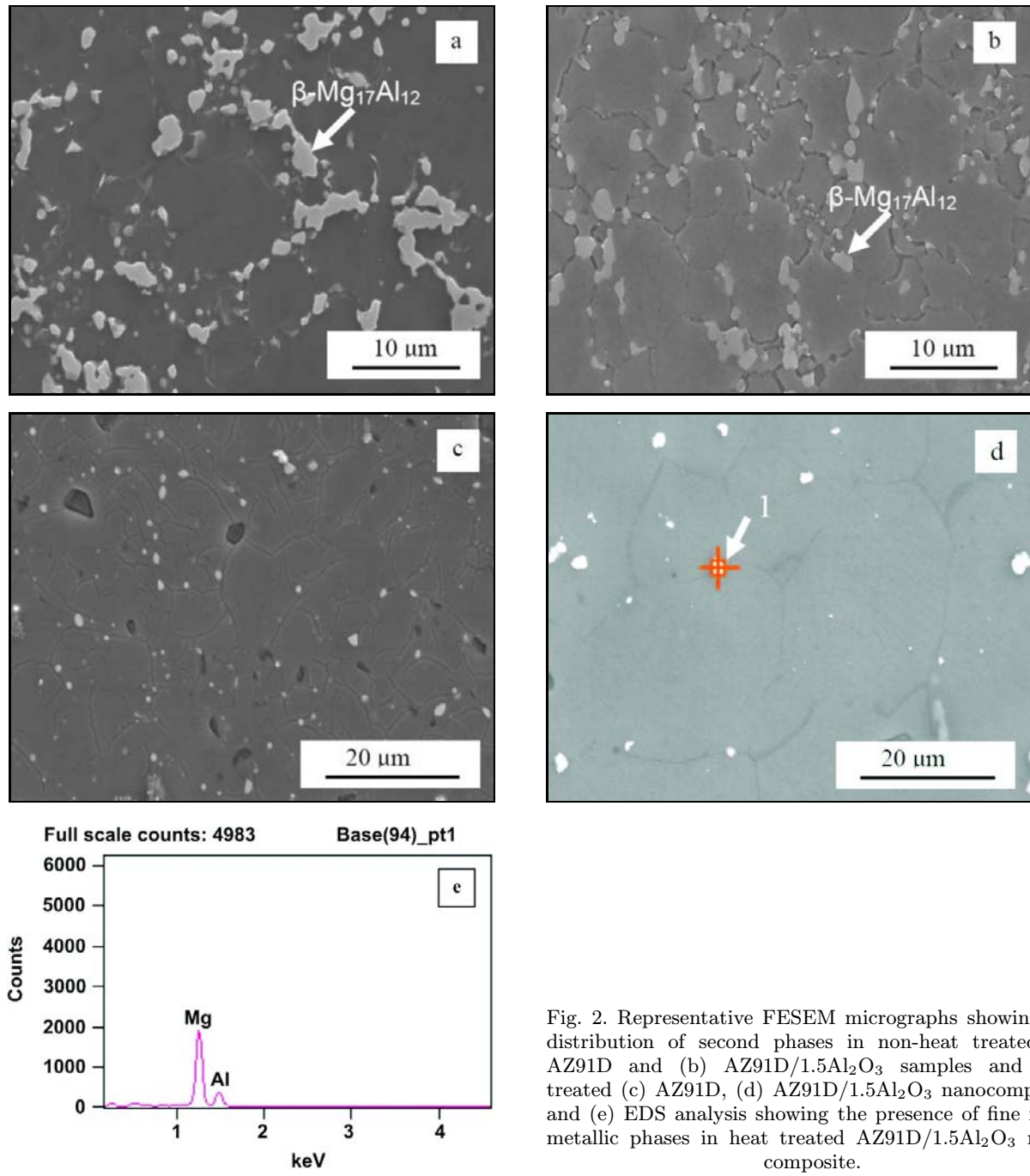

Fig. 2. Representative FESEM micrographs showing the distribution of second phases in non-heat treated (a) AZ91D and (b) AZ91D/1.5Al_2O_3 samples and heat treated (c) AZ91D, (d) AZ91D/1.5Al_2O_3 nanocomposite and (e) EDS analysis showing the presence of fine intermetallic phases in heat treated AZ91D/1.5Al_2O_3 nanocomposite.

3.5. Microhardness

The results of microhardness measurements conducted on the polished samples of AZ91D and AZ91D/Al_2O_3 nanocomposites revealed the increasing trend of average microhardness (Table 3) with an increase in amount of nano-alumina particulates in the matrix.

3.6. Tensile characteristics

Results of the ambient temperature tensile tests revealed an improvement in 0.2 % yield strength, ultimate tensile strength, ductility and work of fracture of AZ91D/Al_2O_3 nanocomposites under non-heat treated condition due to the addition of Al_2O_3 nanoparticulates to the matrix (Table 3). The increasing trend of overall tensile properties of nanocomposites with an increase in addition of nano-alumina particulates was also observed. The tensile results of nanocomposites under heat treated condition revealed improved ultimate tensile strength and significantly enhanced ductility and work of fracture (Table 4). However, considering the standard deviation, sim-

Table 2. Results of grain characteristics of non-heat treated and heat treated AZ91D and AZ91D/Al_2O_3 nanocomposites

Material	Grain characteristics (non-HT)		Grain characteristics (HT)	
	Size (μm)	Aspect ratio	Size (μm)	Aspect ratio
AZ91D	6.6 ± 1.9	1.4 ± 0.3	14.3 ± 4.6	1.5 ± 0.3
AZ91D/1.0Al_2O_3	6.5 ± 1.3	1.4 ± 0.3	18.2 ± 5.9	1.4 ± 0.3
AZ91D/1.5Al_2O_3	6.3 ± 2.1	1.4 ± 0.3	18.1 ± 7.6	1.4 ± 0.3

Table 3. Results of room temperature tensile properties of non-heat treated AZ91D and AZ91D/Al_2O_3 nanocomposites

Specimen	Microhardnes, HV	0.2 % YS (MPa)	UTS (MPa)	Ductility (%)	Work of fracture (MJ m^{-3})
AZ91D	102 ± 4	124 ± 13	229 ± 17	9.0 ± 2.0	19.0 ± 4.0
AZ91D/1.0Al_2O_3	119 ± 4	130 ± 13	243 ± 21	9.8 ± 1.8	21.0 ± 4.5
AZ91D/1.5Al_2O_3	135 ± 6	139 ± 9	255 ± 11	13.8 ± 1.6	33.5 ± 5.4
AZ91D/10SiC (7 μm)*	–	135	152	0.8	–

* Reference [14]

Table 4. Results of room temperature tensile properties of heat treated AZ91D and AZ91D/Al_2O_3 nanocomposites

Material	0.2 % YS (MPa)	UTS (MPa)	Ductility (%)	Work of fracture (MJ m^{-3})
AZ91D	85 ± 6	141 ± 14	4.0 ± 1.0	5.0 ± 2.0
AZ91D/1.0Al_2O_3	95 ± 4	221 ± 9	26.0 ± 5.0	51.0 ± 9.0
AZ91D/1.5Al_2O_3	79 ± 6	217 ± 6	31.0 ± 2.0	59.0 ± 6.0
AZ91D/15 SiC (15 μm)*	134 ± 2	204 ± 3	1.2 ± 0.1	–

* Reference [25]

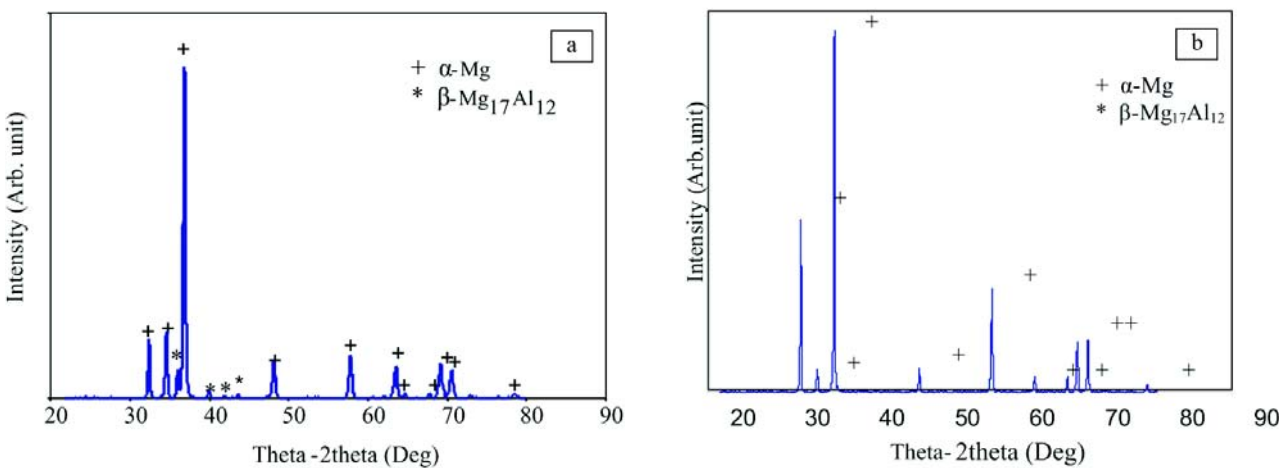

Fig. 3. X-ray diffractogram of: (a) non-heat treated and (b) heat treated AZ91D/1.5Al_2O_3 nanocomposites.

ilar level of 0.2 % yield strength was observed in heat treated unreinforced and reinforced AZ91D magnesium samples (Table 4). For both AZ91D alloy and its nanocomposites, non-heat treated samples showed higher yield and ultimate tensile strength when compared to heat treated samples. On the other hand, composite samples under heat treated condition revealed superior ductility and work of fracture enhancement compared to non-heat treated nanocomposites (Table 4).

3.7. Fracture behaviour

Fracture surface of non-heat treated AZ91D mag-

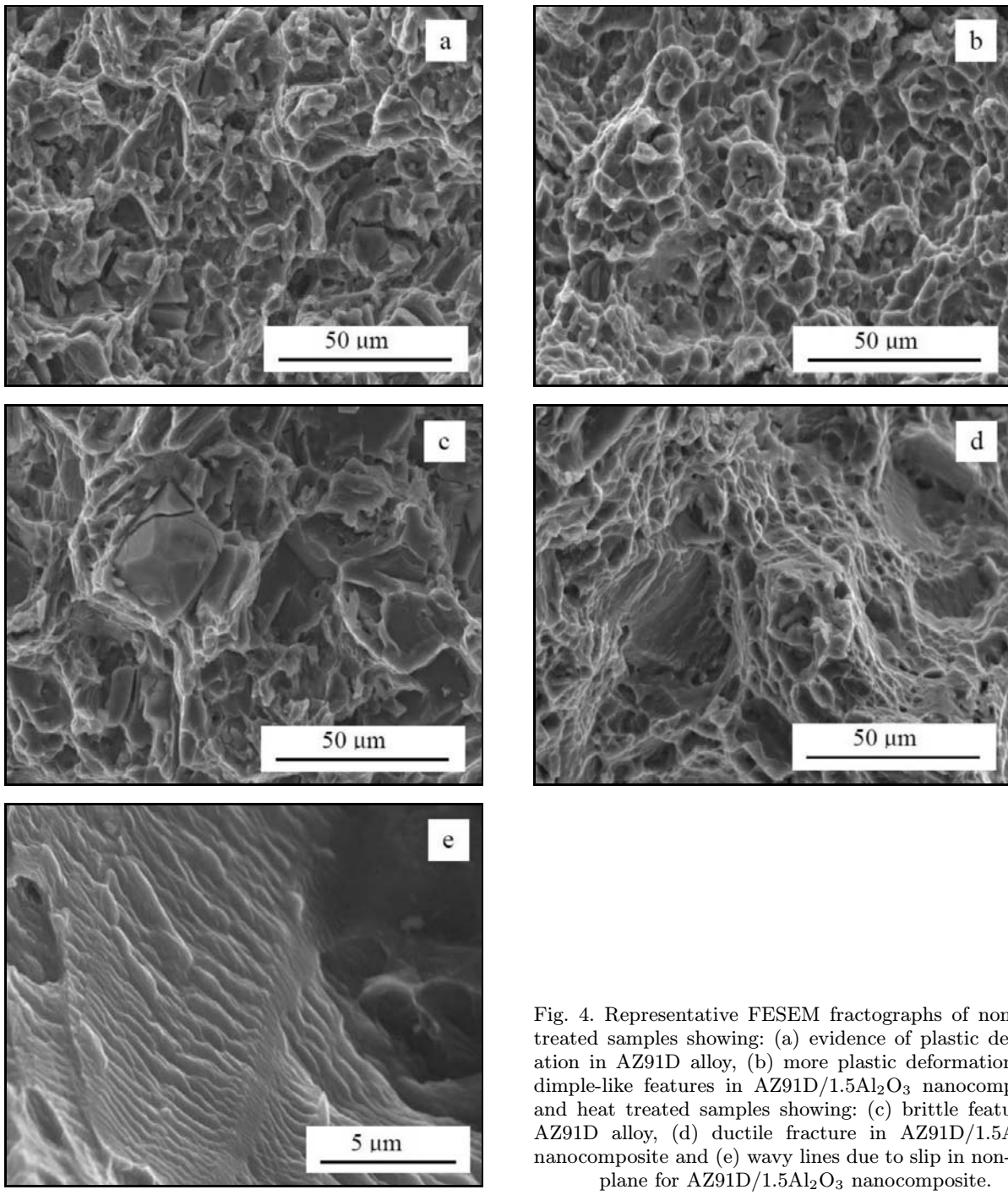

Fig. 4. Representative FESEM fractographs of non-heat treated samples showing: (a) evidence of plastic deformation in AZ91D alloy, (b) more plastic deformation and dimple-like features in AZ91D/1.5Al_2O_3 nanocomposite and heat treated samples showing: (c) brittle feature in AZ91D alloy, (d) ductile fracture in AZ91D/1.5Al_2O_3 nanocomposite and (e) wavy lines due to slip in non-basal plane for AZ91D/1.5Al_2O_3 nanocomposite.

nesium alloy revealed a mixed ductile and brittle fracture mode. However, in case of nanocomposites, the presence of dimple-like features with more plastic deformation was observed with increase in nanoparticulate addition (Fig. 4b). For heat treated samples, microscopically rougher fracture surface with intragranular crack in the matrix was evident in AZ91D alloy (Fig. 4c). However, finer dimple-like features (Fig. 4d) and wavy lines (Fig. 4e) showing activation of non-basal slip in the matrix alloy was evident showing ductile fracture mode in heat treated nanocomposites.

4. Discussion

4.1. Microstructural characterization

Microstructural characterization under non-heat treated condition of AZ91D magnesium alloy and AZ91D/Al_2O_3 nanocomposites revealed that eutectic β-$Mg_{17}Al_{12}$ secondary phases are predominantly located at the grain boundaries as shown in Fig. 2a,b. However, the presence of alumina particulates assisted in breaking down the network of secondary phases

present along the grain boundaries resulting in discontinuous distribution of the phases in the matrix as evident in Fig. 2b. Table 2 shows the effect of nano-alumina particulate addition on the grain size of AZ91D magnesium alloy. It was observed that an increase in addition of nano-alumina particulate to the matrix did not result in grain refinement. This suggests the incapability of the nano-size alumina particulates to serve as either nucleation sites or obstacles to grain growth during solid state cooling. The presence of minimal porosity in the composite materials was supported by nearly theoretical experimental density (Table 1). The reason for such observation can be related to the good compatibility between AZ91D magnesium alloy and alumina particulates and appropriate selection of experimental parameters during processing.

The reasonably uniform distribution of the alumina reinforcement observed in AZ91D/1.5vol.% Al_2O_3 nanocomposites (Fig. 1a) can be primarily attributed to: (1) limited agglomeration of reinforcement in the matrix during melting, (2) good wettability between the matrix and reinforcement [18], and (3) proper extrusion parameters [15, 16]. Density measurements exhibiting almost zero standard deviation also support the uniform distribution of the reinforcement in the melt. Interfacial integrity between the matrix and reinforcement was observed to be good as shown in Fig. 1b and was assessed in terms of interfacial debonding and microvoids at the particulate--matrix interface. This good interfacial integrity can also be due to limited matrix-reinforcement reaction.

After heat treatment, the grain size of AZ91D magnesium alloy and its nanocomposites increased due to the grain growth with an increase in temperature as evident in Table 2. Eutectic secondary phase (β-$Al_{12}Mg_{17}$) was relatively refined and uniformly distributed in monolithic AZ91D magnesium alloy as shown in Fig. 2c. In case of nanocomposites, the secondary phases were limited and discontinuously distributed in the matrix. This is because, according to the Mg-Al equilibrium phase diagram, solution heat treatment carried out at 413 ℃ for 2 h causes the β-$Al_{12}Mg_{17}$ secondary phase to dissolve partially into the α-Mg phase and after quenching to room temperature the remaining secondary phases can be found as finer phases in case of AZ91D alloy and its nanocomposites. Similar dissolution of intermetallic phase due to heat treatment was reported earlier in AZ91D magnesium alloy [19]. X-ray diffraction studies also support the partial dissolution of β-$Al_{12}Mg_{17}$ secondary phase in heat treated AZ91D/1.5Al_2O_3 nanocomposites as shown in Fig. 3. Under heat treated condition (Fig. 3b), the complete disappearance of peaks matching to the β-$Al_{12}Mg_{17}$ secondary phase was observed when compared to the non-heat treated condition (Fig. 3a) in AZ91D/1.5Al_2O_3 nanocomposite. This suggests that the secondary phase (β-$Al_{12}Mg_{17}$) is almost dissolved and is present in low volume fraction ($< 2\,\%$) (as seen in Fig. 3d) after heat treatment in AZ91D/1.5Al_2O_3 nanocomposite.

4.2. Mechanical behavior

The results of hardness measurements revealed that the addition of nano-alumina reinforcement led to a significant increase in microhardness (Table 3) of non-heat treated AZ91D magnesium alloy and can be attributed primarily to: (a) the presence of harder Al_2O_3 particulates in the matrix [16, 20] and (b) a higher constraint to the localized matrix deformation during indentation due to presence of Al_2O_3 particulates.

The results of tensile tests of non-heat treated nanocomposites revealed an improvement in average values of 0.2 % YS, UTS, ductility and work of fracture with increasing amount of nano-alumina reinforcement in the matrix (Table 3). The improvement in strength can be related to: a) CTE mismatch between the Al_2O_3 particulates and AZ91D matrix and an increase in dislocation density in the matrix due to the presence of alumina particulates, b) ability of the matrix to transfer load to the stronger and reasonably distributed Al_2O_3 particulates and c) Orowan strengthening effect due to the presence of nano-alumina particulates. The improvement of strength by alumina particulates at nano-length scale has been supported by earlier findings [20, 21].

The results of tensile testing also revealed an improved ductility exhibited by the nanocomposites when compared to pure AZ91D alloy. This can be attributed to the ability of nano-Al_2O_3 particulates in the matrix to activate non-basal slip at room temperature [22] and presence of discontinuously distributed secondary phases in the matrix. For monolithic AZ91D magnesium alloy, the hard secondary phases are aggregated near the grain boundaries resulting in poor ductility. However, in case of nanocomposites, the addition of nano-alumina particulates assisted in breaking down the aggregation of the secondary phases enabling it to get dispersed in the matrix thus enhancing ductility. The enhancement in ductility due to the breakdown of the secondary phases in the grain boundaries and the distribution of highly aggregated to fine dispersed secondary phases has been established before [23, 24]. Work of fracture of the nanocomposites was found to be improved compared to pure AZ91D alloy. This can be primarily related to the improved strength (0.2 % YS and UTS) and failure strain of the nanocomposites.

After heat treatment, the results of the tensile tests of AZ91D/Al_2O_3 nanocomposites revealed a significant increase in ductility, improved UTS and comparable yield strength to AZ91D alloy (Table 4). The en-

hancement in ductility can be attributed to the presence of limited and discontinuously distributed secondary phases in the microstructure compared to the uniformly distributed secondary phases in the matrix alloy (Fig. 2c,d). The work of fracture of the nanocomposites was also found to increase significantly compared to that of the AZ91D magnesium alloy. The improvement was observed to be ∼ 12 times higher in AZ91D/1.5Al_2O_3 composites samples. This can be related to the improved failure strain exhibited by the heat treated nanocomposites leading to enhanced energy absorbing capability of nanocomposites.

Table 3 shows the comparison of results of tensile tests between the non-heat treated AZ91D/1.5Al_2O_3 nanocomposites and AZ91D/10SiC_P composites. It was observed that the addition of nano-Al_2O_3 particulates to AZ91D matrix has resulted in enhanced strength and ductility compared to AZ91D/10SiC_P composites.

The results of the tensile test of the heat treated (solutionized) AZ91D/1.5Al_2O_3 nanocomposites (Table 4) further showed an enhancement of 125 % ductility and 75 % work of fracture values with sacrifice in strength compared to non-heat treated AZ91D/1.5Al_2O_3 composites. However, when compared to heat treated AZ91D/15SiC_P composites [25], solutionized AZ91D/1.5Al_2O_3 nanocomposites showed excellent ductility, comparable UTS with compromise in yield strength.

4.3. Fracture behaviour

Fracture analysis conducted on tensile fracture samples of non-heat treated AZ91D magnesium alloy revealed the mixed ductile and brittle mode fracture with the evidence of plastic deformation (Table 3). However, the fracture surface in the case of nanocomposite sample revealed a comparatively more ductile mode of fracture with evidence of more plastic deformation such as presence of dimple-like features (Fig. 4b). The change in fracture mode in the magnesium matrix can be attributed to the presence of nano-Al_2O_3 particulates because they provide sites to open cleavage cracks halting an advancing crack front and thus alter the local effective stress from plane strain to plain stress in the neighborhood of crack tip [23] and activation of non-basal slip system at room temperature in magnesium matrix. These features are consistent with the improved ductility exhibited by the nanocomposites.

After heat treatment, the fracture surface of AZ91D magnesium alloy exhibited matrix cracking and microscopically rougher surface compared to the non-heat treated AZ91D magnesium alloy. This explains the inferior ductility exhibited by the heat treated AZ91D alloy (∼ 4 %). Fracture surface of the heat treated AZ91D/1.5Al_2O_3 nanocomposites revealed a predominantly ductile type fracture with presence of fine dimple-like features and activation of non-basal slip plane (Fig. 4e) due to presence of nano-Al_2O_3 particulates and refined secondary phase in low volume fraction in the matrix. This observation is consistent with the tensile results which revealed enhanced ductility in heat treated nanocomposites compared to heat treated and non-heat treated AZ91D magnesium alloy and non-heat treated nanocomposites.

5. Conclusions

1. Disintegrated melt deposition technique coupled with hot extrusion can be used to synthesize nano-Al_2O_3 particulates reinforced AZ91D magnesium alloy composites.

2. Microstructural characterization of non-heat treated nanocomposites revealed reasonably uniform reinforcement distribution with good interfacial integrity and discontinuously distributed secondary phases. After heat treatment, the microstructural characterization of the nanocomposites revealed increased matrix grain size and the presence of finer and discontinuously distributed secondary phases throughout the matrix.

3. The results of the tensile tests of non-heat treated nanocomposites revealed improvement in hardness, 0.2 % YS, UTS, ductility and work of fracture. After heat treatment, significant enhancement in ductility was observed in nanocomposites with compromise in strength compared to non-heat treated composites.

4. Fractography revealed that fracture behavior of non-heat treated AZ91D magnesium alloy changed from mixed ductile and brittle fracture to a relatively more ductile type fracture in nanocomposites due to the presence of nano-alumina particulates. Fracture behavior of heat treated AZ91D/Al_2O_3 nanocomposites revealed dominantly ductile type fracture with finer dimple-like features and evidence of wavy lines showing non-basal slip activation arising due to solution heat treatment at high temperature and presence of nano-alumina particulates in the matrix.

Acknowledgements

Authors wish to acknowledge National University of Singapore for funding this research through grants and studentships, and Agency for Science, Technology and Research (ASTAR) Grant 092 137 0015 (WBS# R-265-000-321-305).

References

[1] DAHLE, A. K.—LEE, Y. C.—NAVE, M. D.—SCHAFFER P. L.—ST JOHN, D. H. J.: Light Metals, *1*, 2001, p. 61. doi:10.1016/S1471-5317(00)00007-9

[2] KIM, J. M.—SHIN, K.—KIM, K. T.—JUNG, W. J.: Scripta Mater, *49*, 2003, p. 687. doi:10.1016/S1359-6462(03)00392-0
[3] POLMEAR, I. J.: Light Alloys, Metallurgy of the Light Metals. London, Edward Arnold 1996.
[4] CLYNE, T. W.—WITHERS, P. J.: An Introduction to Metal Matrix Composites. Cambridge, UK, Cambridge University Press 1993. doi:10.1017/CBO9780511623080
[5] YUAN, G. Y.—SUN, Y. S.—DING, W. J.: Mater Sci Eng A, *308*, 2001, p. 38.
[6] HIRAI, K.—SOMEKAWA, H.—TAKIGAWA, Y.—HIGASHI, K.: Mater Sci Eng A, *403*, 2005, p. 276. doi:10.1016/j.msea.2005.05.028
[7] WU, G.—FAN, Y.—GAO, H.—ZHAI, C.—ZHU, Y. P.: Mater Sci Eng A, *408*, 2005, p. 255. doi:10.1016/j.msea.2005.08.011
[8] ZHAO, Z.—CHEN, Q.—WANG, Y.—SHU, D.: Mater Sci Eng A, *515*, 2009, p. 152. doi:10.1016/j.msea.2009.03.030
[9] AMBAT, R.—AUNG, N. N.—ZHOU, W.: Corros Sci, *42*, 2000, p. 1433. doi:10.1016/S0010-938X(99)00143-2
[10] AUNG, N. N.—ZHOU, W.: J Appl Electrochem, *32*, 2000, p. 1397. doi:10.1023/A:1022698916817
[11] BAG, A.—ZHOU, W.: J Mater Sci Lett, *20*, 2001, p. 457. doi:10.1023/A:1010919017805
[12] KAGAWA, Y.—NAKATA, E.: J Mater Sci Lett, *11*, 1992, p. 176. doi:10.1007/BF00724684
[13] LLORCA, N.—BLOYEE, A.—YUE, T. M.: Mater Sci Eng, *135A*, 1991, p. 247.
[14] LUO, A.: Metall Mater Trans, *26A*, 1995, p. 2445.
[15] LLOYD, D. J.: Int Mater Rev, *39*, 1994, p. 1.
[16] GUPTA, M.—LAI, M. O.—SARAVANARANGANATHAN, D.: J Mater Sci, *35*, 2000, p. 2155. doi:10.1023/A:1004706321731
[17] AVEDESIAN, M. M.—BAKER, H. (Eds.): Magnesium and Magnesium Alloys. In: ASM Specialty Handbook. Materials Park (OH), ASM International, Materials Information Society 1999, p. 79.
[18] EUSTATHOPOULOS, N.—NICHOLAS, M. G.—DREVET, B.: Wettability at High Temperatures. Pergamon Materials Series. Oxford, UK, Elsevier Science Ltd. 1999.
[19] WANG, Y.—LIU, G.—FAN, Z.: Acta Mater, *54*, 2006, p. 689. doi:10.1016/j.actamat.2005.09.033
[20] HASSAN, S. F.—GUPTA, M.: Mater Sci Tech, *20*, 2004, p. 1383. doi:10.1179/026708304X3980
[21] HASSAN, S. F.—GUPTA, M.: J Alloys Compd, *419*, 2006, p. 84. doi:10.1016/j.jallcom.2005.10.005
[22] HASSAN, S. F.—GUPTA, M.: Mater Sci Eng A, *25*, 2006, p. 22. doi:10.1016/j.msea.2006.03.029
[23] DIETER, G. E.: Mechanical Metallurgy, SI Metric Edition. New York, McGraw-Hill Book Company 1988.
[24] NGUYEN, Q. B.—GUPTA, M.: J Alloys Compd, *459*, 2008, p. 244. doi:10.1016/j.jallcom.2007.05.038
[25] PODDAR, P.—SRIVASTAVA, V. C.—DE, P. K.—SAHOO, K. L.: Mater Sci Eng A, *460–461*, 2007, p. 357. doi:10.1016/j.msea.2007.01.052